THERMAL TOMOGRAPHY BASED ON TIME TRANSFORMATION

Ing. Lukáš Muzika,
Západočeská univerzita v Plzni,
Univerzitní 8, 306 14 Plzeň
Česká republika

Ing. Michal Švantner, PhD.,
Západočeská univerzita v Plzni,
Univerzitní 8, 306 14 Plzeň
Česká republika

ABSTRACT

The contribution describes a new algorithm of thermographic evaluation of pulse thermography. The principle is in a time transformation of a thermographic sequence. The technique provides result in one image instead of series of images as standard algorithms do (FFT, TSR, derivation). This makes the evaluation faster and easier for the operator. The result can be sliced to ranges of depths, similar way as in tomography. Thereby, this technique is a part of the family of techniques often referred as thermal tomography. The algorithm is verified experimentally on a Flat Bottom Hole sample 3D-printed from ABS. The principle of slicing is described and showed on real experimental data. The advantages and disadvantages of this technique are discussed in this contribution.

KEYWORDS

Infrared non-destructive testing, pulse thermography, thermal tomography, defect depth estimation

INTRODUCTION

Infrared nondestructive testing (IRNDT) is an inspection technique used in many different field of industry. It is not limited just for defect detection (recognizing if a part of tested object is defective or non-defective) but it is also used in many cases for defect depth, thermal and other properties estimation. Over the past decades many different types of IRNDT was developed and established as standard technique for defect detection in particular area (e.g. lock-in thermography for solar cells testing[1][2][3]). Nonetheless the most popular technique remains pulse thermography, due to fast inspection time and relatively simplistic analytical modelling. By pulse thermography the excitation source (e.g. flash lamp, halogen lamp, laser, electric current) excites the object by one pulse and temperature response on this pulse is than recorded by suitable IR detector (IR camera). Schematic principle of excitation and thermal response recording is in **Fig. 1**.

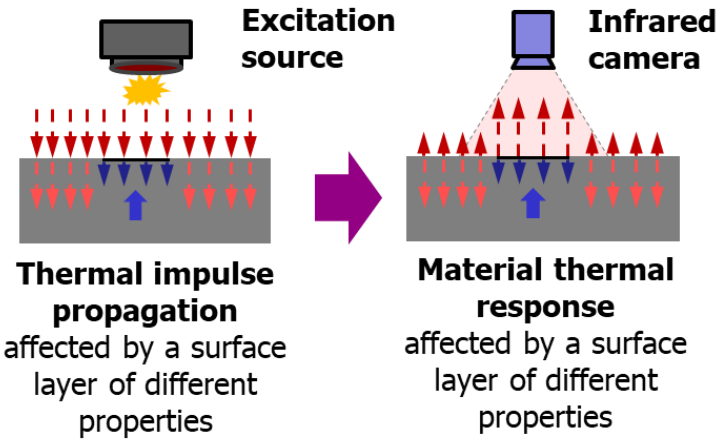

Fig. 13: Composition of IRNDT system

The acquisition process of pulse thermography is always the same. Parameters which can be changed are duration of the recording (number of frames of recorded thermographic sequence) and the speed of acquisition (framerate of IR camera). With some excitation sources (e.g. laser) the pulse length can be also adapted. In the most common combination, the excitation source for pulse thermography is a flash lamp. The pulse length in this case cannot be changed. It is very appealing for operators that just two parameters can be changed and thus the recording part is very simple. The raw thermographic sequence usually must be post-processed to get useful information. Many

different techniques of post-processing were developed and has been used on day to day basis. One of the most popular techniques are Fourier Transform [4] or Wavelet transform [5] based algorithms, techniques based on singular value decomposition [6] and thermographic signal reconstruction [7]. A complexity of the evaluation (post-processing) often limits a usability of the pulse thermography in industrial applications. The results of post-processing are often in a form of a sequence composed from many images (typically more than 1000), which should be inspected manually by an operator. In practice it means that operator is searching for one image in the whole post-processed sequence to detect a defect. If defects are in different depth they appear in different image, which makes the evaluation procedure time demanding. In the worst case the image which shows clearly an indication of defect can be for example missed due to tiredness of the operator. From the mentioned above it is obvious that algorithm which could compress the most important information in just one resulting image would be very beneficial for evaluation in industrial application. Not just the recording part would be easy to do but also the evaluation part.
The proposed technique allows all mentioned above. It is based on analyses of an artificial function obtained by multiplying a front-surface temperature evolution by the power function of time $T(\tau) \times \tau^n$ thereby we call it time power transformation or shortly P-function. The advantage of this technique is that the result is in form of one image. This is beneficial for reduction of time needed for evaluation by the operator (he or she doesn't have to search indications in the sequence). Furthermore, P-function allows to display ranges of depth of material (e.g. from depth 1-1.5 mm), similar way as in tomography. P-function is thus a part of the family of techniques often referred as thermal tomography. In [8] there is a review of some of them. Many of them are not usable in real industrial application because they need perfect raw sequence (sequence without noise and high signal to noise ratio for each defect) which shall be processed.

P-FUNCTION

The technique is based on time transformation. The time transformation approach was introduced and further improved in [8][9][10][11]. Nonetheless, the approach was verified mostly on analytical data obtained from some simulation software and when tested on real data it did not perform that well. Thereby some changes were done by us to improve the performance for measured data. By P-function, a de-noised front-surface temperature evolution is multiplied by the power function of time $T(\tau) \times \tau^n$. The resulting curve contains easily detectable variations. Those points occur in certain time (τ_{inx}), which is dependent on defects depth. We can find characteristic point via searching for minimum. The time of occurrence of this point is than set as the result in resulting image (timegram).

There are two big differences in our approach compared to previous publications [9][10][11]. Firstly, the data are de-noised, because the noise may vary the minimum and thus the characteristic time. There are several options how to lower noise. Two possibilities seems suitable for this purpose – using filter or fit data with artificial function. The filtering approach may seem easier but it is complicated task especially when it should be universal (use for different materials with different amount of noise). Our tests shows that in many cases filter doesn't remove enough noise or it significantly lowers the noise, nonetheless it creates some additional peaks. It should be noted that we tried moving average filtering, Savitzky-Golay filtering and locally weighted scatter plot smoothening available in Matlab. It is not excluded that another type of filter could provide good results.
For data fitting and thus noise reduction we use function **(1).**

$$T(t) = A \cdot \ln(t)^5 + B \cdot \ln(t)^4 + C \cdot \ln(t)^3 + D \cdot \ln(t)^3 + E \cdot \ln(t)^2 + F \cdot \ln(t) + G \qquad (1)$$

Where A, B, C, D, E, F and G are coefficients to be fitted. The function is similar to function used for TSR [7] except instead of base 10 logarithm, the natural logarithm is used.
The second big difference is that for determination of characteristic time we use searching for minimum instead of searching for inflexion points. The reason to do so is that several inflexion points can occur on the resulting curve. It is not easy task to determine which inflexion point should be chosen, if the process should be automatic.

EXPERIMENTAL PART

The experiments were performed on sample, which was printed by 3D printer from ABS. The sample has dimensions 95x70x9 mm and contains 6 defects with diameter 5 mm. The sample is a standard Flat Bottom Hole sample. The remaining wall thickness is for defects 1-6: 0.2, 0.6, 1, 1.4, 1.8 and 2.2 mm. The sectional view of defect 1-3 is for clarity in **Fig 2**.

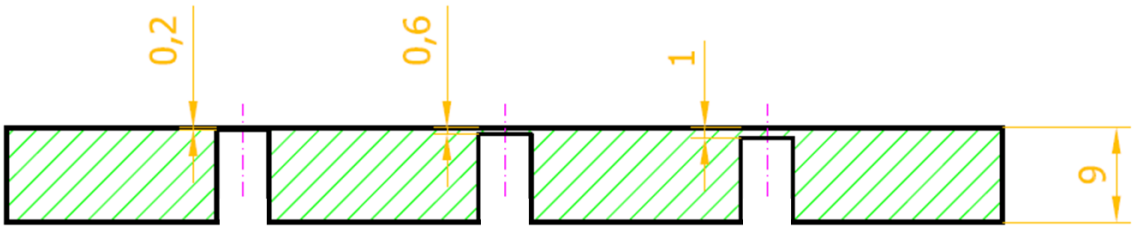

Fig. 14: Visualization of the sample (Defect 1-3)

The data were recorded by IR camera FLIR SC7650. The framerate of camera was set to 30 Hz and 1500 frames were recorded.

The most challenging problem for the time transformation is to choose suitable parameter (the n from time transformation). Our solution is to calculate the result for several n. We vary n from 0.01 till 0.4 with the step 0.03. After the best n is chosen, we do it by calculating CNR (more about CNR can be found in [12]) for defects on which we are focused but it can be done just by eye, we proceed to fine tuning. E.g. if we get the best result at 0.04, we do the calculation again from 0.02 till 0.06 with step 0.01 and we chose the best result. We basically chose n experimentally. The best approach for choosing n may vary based on the power of a PC and an optimization of a software used for the calculation. In general, the calculation of power function is fast, it should be noted that the most time demanding part is the de-noising procedure. The advantage is that when the suitable n is chosen for the material and the defect, it is always the same. This is well suited for serial testing. For 3D printed sample the best parameter was 0.03.

The temperature response from defect 3 is shown in **Fig. 3**. As it can be seen on fitted data, the fit is very precise and furthermore there isn't any noise in the curve.

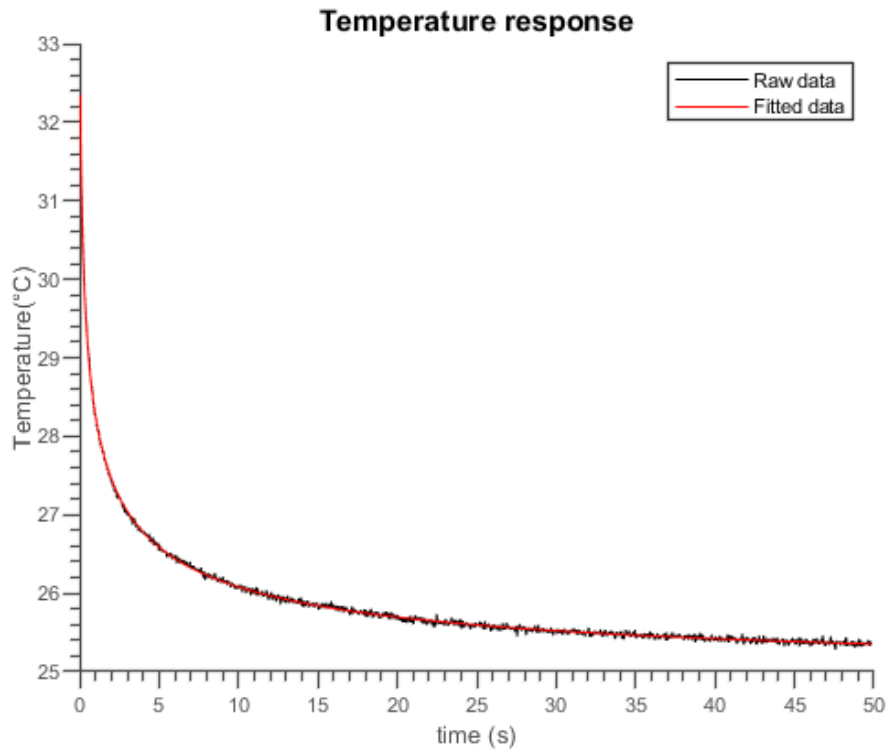

Fig. 15: Temperature response on a pulse and its fitting

The P-function curve from defect 3 is in **Fig. 4**. The parameter of time transformation was set to 0.03. The characteristic point and thus characteristic time can be easily find via minimum search.

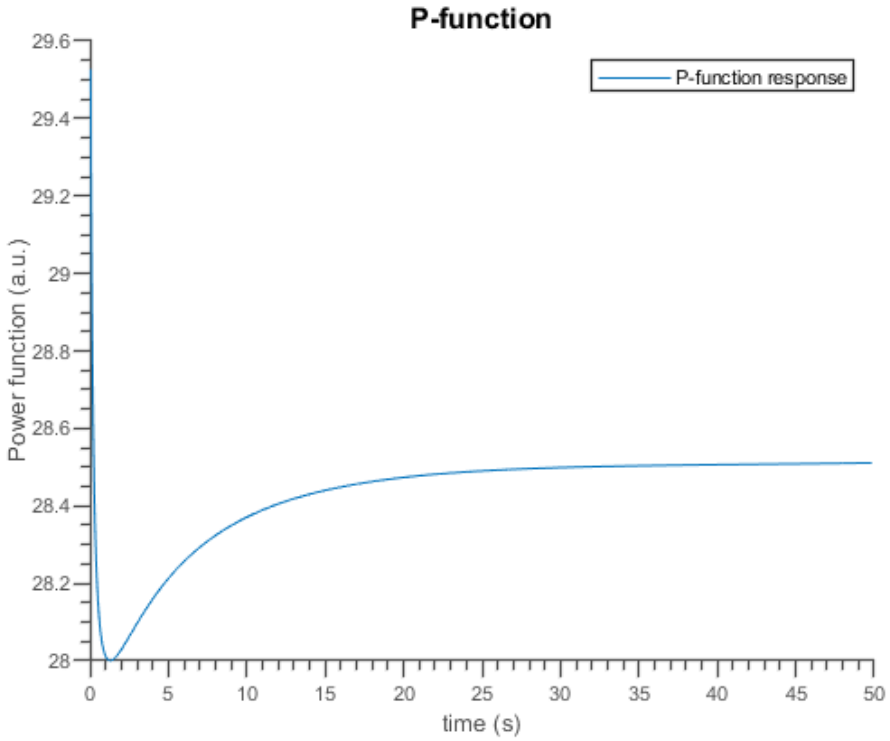

Fig. 16: P-function curve, defect 3, parameter 0.03

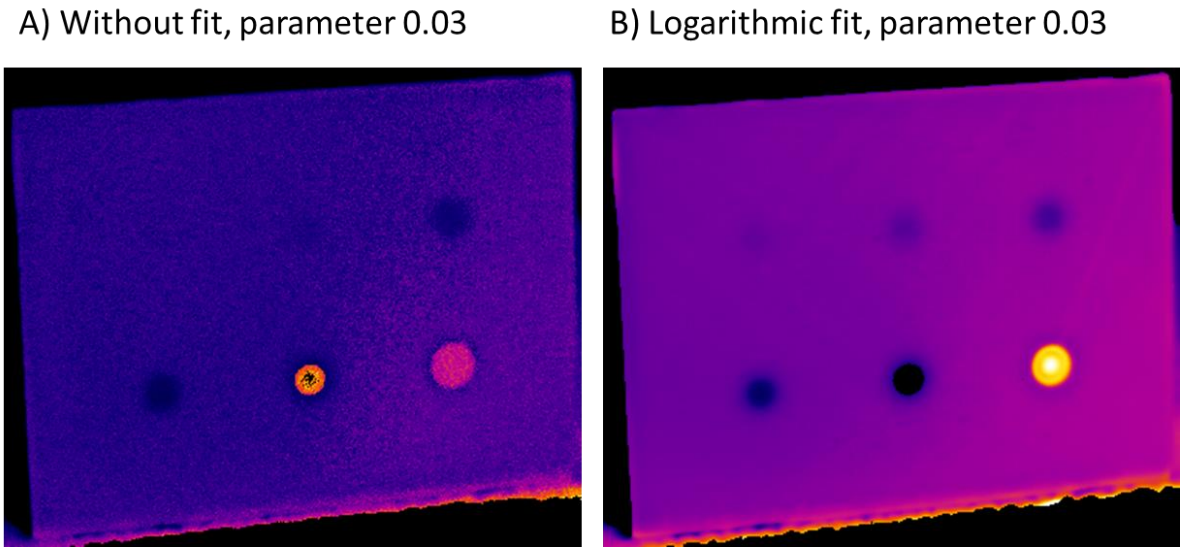

Fig. 17: Comparison of timegrams with and without de-noising

Timegrams without fitting and with fitting are shown in **Fig. 5** (with parameter 0.03). The timegram without any fitting shows less indications than the timegram with fitting. The result also appears noisier. This noise can be seen on the non-defective part of the sample, where non-defective pixels are not the same (difference between right side and left side, visible grains in the timegram). The noise in timegram is caused by the noise of raw data. When the noisy temperature response is time transformed, the characteristics points can shift and thus cause even more noise in resulting image. The timegram without fit shows just 4 of the defects. The P-function is without de-noising usable just on high quality sequences without noise. It actually means this option is not usable in practical application. Timegram where fitting preceded provides indications of all defects. The non-defective pixels are indistinguishable to each other. No apparent noise is detectable in the timegram. The only disadvantage is that computation time is longer due to the de-noising.

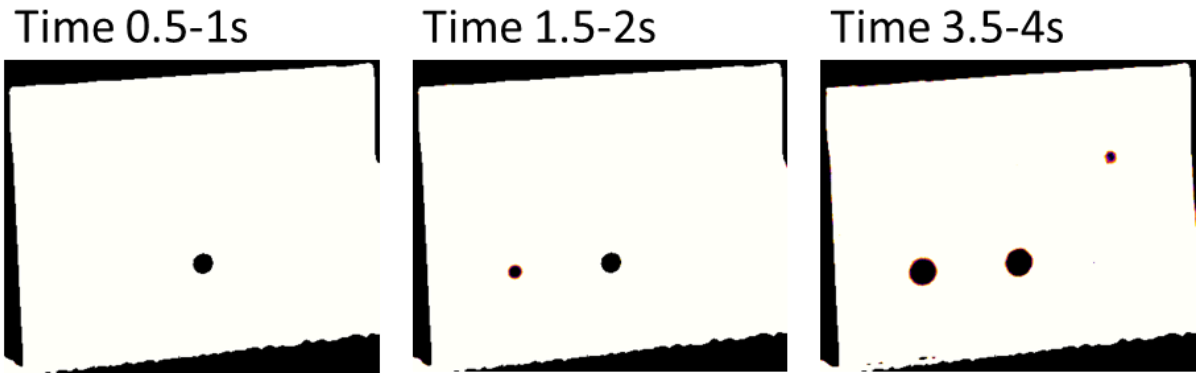

Fig. 18: Slicing to different defect depth

The slicing to interval of depths is demonstrated in **Fig. 6** on three examples (three different levels of depth). The slicing is performed via setting specific range of τ_1 and τ_2 which corresponds to depth z_1 and z_2. The lower time means lower depth. That's why in range 0.5-1 s we can distinguish just the defect 2, which has second lowest remaining wall thickness. With increasing time, we can see defects which have higher remaining wall thickness. When some defect occurs it is then visible in all ranges. This is actually expected result, because all of the defect are flat bottom hole and thus in each slices they should be the same. This demonstrates that the slicing actually works. Defect 1 is not visible before defect 2 due to overheating in area of defect 1 compared to different defects. With different parameter we could reach result where the assumption longer characteristic time means deeper defect is fulfilled nonetheless just defect 1 would be visible. Actually different behavior of defect1 is not an issue

for detecting of an indication, because the indication of defect 1 is visible in **Fig. 5** but it is problematic for defect depth estimation because the characteristic time is shifted beyond characteristic time of non-defective area.

CONCLUSION

In this contribution thermal tomography based on time transformation was described. The P-function algorithm is easy to implement and provides interesting results. The biggest advantage is possibility of slicing (setting the range) result to different depth from which you can see which defects are closer to the surface. Other techniques allow similar possibility via browsing the whole resulting sequence (e.g. blind frequency approach in pulse phase thermography), where the disadvantage is the need to go through sequence compared to use one image with P-function. The advantage of just one resulting image is especially suitable for some type of machine learning, where it is easier to analyze just one image and even for operator, who doesn't need to go through resulting sequence, which saves time and improves reliability.

The applicability of P-function was verified on measured thermographic sequence. The biggest problem for applicability is noise, which we suppress via fitting. The parameter of P-function significantly influences the results. We weren't focused on finding some relationship to get parameter via equation, which is to be one of next part of our research in this field. We believe that for practical purposes experimental searching for parameter is sufficient due to the fact, when parameter is once found, it doesn't change for the same material and thus is searched for just the first time. This advantage is lost when P-function should be used just for one-time measurement of some object. In that case we don't see any difference between going through resulting sequence of e.g. phasegrams (pulse phase thermography) or timegrams with different parameters (in that case sequence of timegrams is created due to different parameters).

P-function has some interesting features and could be applicable in wide variety of application.

ACKNOWLEDGMENTS

The work has been supported by the Ministry of Education, Youth and Sports of the Czech Republic within the OP RDI programme, CENTEM project, no. CZ.1.05/2.1.00/03.0088, co-funded by the ERDF; and National Sustainability Programme I., CENTEM PLUS project, no. LO1402 and by project SGS-2019-008.

REFERENCES

[1] O. Breitenstein, "Illuminated versus dark lock-in thermography investigations of solar cells," *Int. J. Nanoparticles*, vol. 6, no. June 2012, pp. 81–92, 2013.

[2] O. Breitenstein *et al.*, "Can luminescence imaging replace lock-in thermography on solar cells and wafers?," in *2011 37th IEEE Photovoltaic Specialists Conference*, 2011, vol. 1, no. 2, pp. 159–167.

[3] L. Muzika, M. Švantner, and M. Kučera, "Lock-in and pulsed thermography for solar cell testing," *Appl. Opt.*, vol. 57, no. 18, pp. 90–97, 2018.

[4] C. Ibarra-castanedo, "Quantative subsurface defect evaluation by Pulsed Phase Thermography," p. 188, 2005.

[5] M. H. Karimi and D. Asemani, "Surface defect detection in tiling Industries using digital image processing methods: Analysis and evaluation," *ISA Trans.*, vol. 53, no. 3, pp. 834–844, 2014.

[6] R. Hidalgo-Gato, J. R. Andrés, J. M. Lopez-Higuera, and F. J. Madruga, "Quantification by Signal to Noise Ratio of Active Infrared Thermography Data Processing Techniques," *Opt. Photonics J.*, 2013.

[7] D. L. Balageas, J.-M. Roche, F.-H. Leroy, W.-M. Liu, and A. M. Gorbach, "The thermographic signal reconstruction method: A powerful tool for the enhancement of transient thermographic images," *Biocybern. Biomed. Eng.*, vol. 35, no. 1, pp. 1–9, 2015.

[8] V. P. Vavilov, D. A. Nesteruk, V. V. Shiryaev, A. I. Ivanov, and W. Swiderski, "Thermal (infrared) tomography: Terminology, principal procedures, and application to nondestructive testing of composite materials," *Russ. J. Nondestruct. Test.*, vol. 46, no. 3, pp. 151–161, 2010.

[9] V. P. Vavilov, "NDT & E International Dynamic thermal tomography : Recent improvements and applications," *NDT E Int.*, vol. 71, pp. 23–32, 2015.

[10] V. P. Vavilov and S. S. Pawar, "Test method A novel approach for one-sided thermal nondestructive testing of composites by using infrared thermography," *Polym. Test.*, vol. 44, pp. 224–233, 2015.

[11] V. P. Vavilov and M. V. Kuimova, "Dynamic Thermal Tomography of Composites: A Comparison of Reference and Reference-Free Approaches," *J. Nondestruct. Eval.*, vol. 38, no. 1, 2019.

[12] M. Švantner, L. Muzika, T. Chmelík, and J. Skála, "Quantitative evaluation of active thermography using contrast-to-noise ratio," *Appl. Opt.*, vol. 57, no. 18, p. D49, 2018.